Supplementary Materials

Pablo SÁNCHEZ-GÁMEZ[*1], Francisco J. NAVARRO[1], Toby J. BENHAM[2],
Andrey F. GLAZOVSKY[3], Robin P. BASSFORD[4], Julian A. DOWDESWELL[2]

[1]*Departamento de Matemática Aplicada a las TIC, ETSI Telecomunicación, Universidad Politécnica de Madrid, Madrid, Spain*
[2]*Scott Polar Research Institute, University of Cambridge, Cambridge, UK*
[3]*Institute of Geography, Russian Academy of Sciences, Moscow, Russia*
[4]*Hardenhuish School, Chippenham, Wiltshire, UK*
[*]*E-mail: pablo.sgamez@upm.es*

ABSTRACT.

1. Further information on climatic conditions on Severnaya Zemlya and the Academy of Sciences Ice Cap

Zhao and others (2014) have shown that NCEP-NCAR reanalysis summer temperatures over Severnaya Zemlya have weak correlations with Golomyanny Island station-measured summer mean temperatures. They note that Golomyanny Island station is located within the Severnaya Zemlya archipelago 130 km away from the ice cap to the southwest into the Kara Sea (Fig. 1b), at only 7 m a.s.l., and is strongly influenced by the ocean environment due to sea-ice melting in summer. On the other hand, Opel and others (2009) found no correspondence between the number of melt layers in the ice core drilled at the Academy of Sciences Ice Cap summit and the Golomyanny station summer surface air temperatures. Furthermore, Zhao and others (2014) found that the total number of melt days on Severnaya Zemlya was strongly correlated with NCEP-NCAR reanalysis summer temperatures. These findings therefore question the use of Golomyanny Station temperature data, which we will avoid in our analysis.

An automatic weather station installed close to the summit of Academy of Sciences Ice Cap between May 1999 and May 2000 provided temperature information for the air and the shallow snow (Kuhn, 2000). The mean annual air temperature was -15.7 °C, whereas the average temperature of uppermost 10 metres of snow/firn was warmer at -10.2 °C, because of the latent heat released by the refreezing of percolating surface meltwater. During the summer months of July and August temperatures were commonly above freezing point causing snowmelt and a decrease in snow height (Kuhn, 2000).

The temperature record from the Academy of Sciences Ice Cap during the last 275 years, inferred from δ^{18}O concentrations in the ice core, showed a minimum in ∼1790 followed by an increasing overall trend up to present but with a double maximum in the first half of the 20th century (Fritzsche and others, 2005; Opel and others, 2013). This increasing temperature trend helps explaining the role of the Kara Sea as a moisture source in the area (Opel and others, 2009; Zhao and others, 2014) as does the increase in sea-salt content at low altitudes on the ice cap, especially during warm summers (Opel and others, 2013). The increase in moisture in the region was also influenced by the decreasing trend of sea-ice cover in the Arctic beginning in the 1980s (Stroeve and others, 2011). The overall picture of temperature change in the last decades is especially critical for the Arctic region, with a tipping point at the beginning of the 1980s (Hansen and others, 2010).

2. Some theories that could explain the velocity variations observed during the winter

We here briefly present other theories that we analysed in an attempt to understand the velocity variations observed during the winter. Among the available studies, we highlight that of Willis (1995), who made a thorough analysis of the physical basis for intra-annual glacier velocity variations, distinguishing between processes operating at the ice-bed interface during the summer and during the winter, and between processes acting on hard-bedded and soft-bedded glaciers. We will focus on the latter, as a soft bed has been suggested for much of the Academy of Sciences ice Cap (Dowdeswell and others, 2002). Following Willis (1995), a theory explaining velocity variations during winter is that a low subglacial water flux will tend to be routed through the till via Darcian flow. Subglacial water pressure will be high and constant bed deformation might occur. However, this cannot explain quasi-oscillatory velocity changes such as those observed in our records (Fig. **??**) . The same applies to theories indicating that an inefficient drainage system, such as a layer of subglacial sediments, might have retained a significant fraction of water throughout the winter months, thereby facilitating continuously high, but diminishing deformation of water-saturated sediments (Tulaczyk and others, 2000; Fischer and Clarke, 2001; Bougamont and others, 2011). Another process suggested by Willis (1995), which could explain non-steady velocity variations, is that periods of accelerating unstable bed deformation may occur temporarily during till failure by liquefaction. An alternative explanation is that rapid variations in fast flow could be caused by changes in associated driving stresses, for example, with changing surface slope due to heterogeneous cumulative snow accumulation during the winter. These possible explanations, however, lack observational support from the available data, and are suggested here for completeness.

3. Possible factors controlling long-term changes and trends in climatic mass balance

Summer air temperature and precipitation are the most evident controlling factors. Using NCEP-NCAR and ERA-Interim reanalysis data for Novaya Zemlya and Severnaya Zemlya from 1995-2011, Zhao and others (2014) have analysed the influence

of summer (June-September) mean 850 hPa geopotential height temperature on snowmelt. They analysed the trends of both total melt days (TMD) and melt offset date (MOD). For Severnaya Zemlya, the temperature trends between 1995-2011 were of $0.80°$C/decade (NCEP-NCAR, p-value < 0.05) and $0.88°$C/decade (ERA-Interim, p-value $= 0.065$). Zhao and others (2014) found a positive correlation between mean TMD and the average June-September NCEP-NCAR air temperature at 850 hPa, with the slope of the linear regression of 10 days $°C^{-1}$ (r=0.843, p-value < 0.0001). Using simple regression, they also found that Severnaya Zemlya's TMD is significantly anti-correlated to the Laptev Sea (r=-0.735, p-value < 0.001) and Kara Sea (r=-0.678, p-value < 0.003) September sea-ice extent. However, since sea-ice extent and glacier surface melting can co-respond to the regional temperature increase, Zhao and others (2014) additionally used partial correlation analysis to remove the large-scale influence of air temperature on both variables. After removing these effects, partial correlation analysis suggested that glacier melt on Severnaya Zemlya was still statistically anti-correlated to the Laptev Sea and Kara Sea sea-ice extent. The explanation is thought to be that reduced offshore sea-ice concentration, i.e. increased open-water fraction, can enhance onshore advection of sensible and latent heat fluxes (Rennermalm and others, 2009). However, even if long-term changes in summer (and annual) temperatures have been observed during our period of analysis (Fig. S3), and regional sea-ice concentration has also shown a clear decreasing trend (Fig. S2), these changes seem have exerted only a minor impact on the long-term climatic mass balance estimates for the Academy of Sciences Ice Cap, which remain close to zero. As noted by Zhao and others (2014), an explanation could be that sea-ice reduction exposes larger areas of open water in summer to evaporation and change the large-scale atmospheric circulation, which has been shown to intensify summer precipitation over the Arctic (Serreze and others, 2012; Francis, 2013).

In particular, the influence of sea-ice concentration on precipitation has been observed for the Academy of Sciences Ice Cap. The analyses by Opel and others (2009) of the deep ice core drilled at the ice cap summit in 1999-2001 has revealed this influence. Deuterium excess (the difference between the two stable water-isotope ratios δ^{18}O and δD) in precipitation depends mainly on evaporation conditions in the moisture source region, and to a lesser degree on condensation temperatures. The main controlling factors are the relative air humidity and the sea-surface temperature (SST) and, to a lesser extent, wind speed during evaporation. Based on the relationship between deuterium excess and SST, Opel and others (2009) noted that in hemispherically warmer periods the Academy of Sciences Ice Cap receives more precipitation from moisture evaporated at lower SSTs, for example due to a northward shift of the moisture source. Since most precipitation on Severnaya Zemlya is brought by air masses moving from the south and southwest, the Kara Sea is likely to be a regional moisture source and its sea-ice cover the main factor influencing summer and autumn evaporation. Lower sea-ice extent in the Kara Sea would allow higher evaporation rates and enhance the contribution of regional moisture to precipitation over the Academy of Sciences Ice Cap. Moholdt and others (2012) have analysed some evidence of this precipitation increase for Novaya Zemlya and Severnaya Zemlya, finding a slightly higher precipitation rate in 2004-2009 with respect to the 1980-2009 mean, especially for Novaya Zemlya. However, the close-to-zero climatic mass balance of Severnaya Zemlya suggests that the recent precipitation anomaly is also likely to be real for this archipelago, as it provides the most reasonable mechanism to counterbalance the observed increasing melt trend. Summarizing, the near-equilibrium climatic mass balance of the Academy of Sciences Ice Cap (and Servernaya Zemlya in general) is probably the result of two opposing effects. On one hand, sea-ice cover loss would enhance precipitation by exposing larger areas of open water to evaporation. On the other, these larger areas of open water would allow onshore advection of heat fluxes from warming mixed ocean layers, accelerating surface melt on the ice cap. With the climatic mass balance remaining near zero, the role of the calving flux is critical in determining the total mass balance of the Academy of Sciences Ice Cap.

4. On the calculation of the shares of total ablation by frontal ablation and surface ablation

Here, additional material is presented supporting the calculation of the total accumulation over the Academy of Sciences Ice Cap, based on the measured net accumulation at the ice cap summit and its variation with altitude.

At the summit, analysis of an ice core detected the layers of maximum radioactivity (in terms of Cesium[137]) corresponding to the 1963 atmospheric nuclear tests and to the 1986 Chernobyl event. The resulting average net accumulation rates were 0.45 m w.e. a^{-1} from 1963 to 1999, and 0.53 m w.e. a^{-1} from 1986 to 1999 (Fritzsche and others, 2002). Later analyses by Fritzsche and others (2005) gave an average accumulation rate of 0.46 m w.e. a^{-1} over 1956-1999 based on stable-isotope investigations. These values were also in agreement with the mean annual net mass balance of 0.43-0.44 w.e. a^{-1} observed by Zagorodnov for 1986/87 using structural-stratigraphic methods; however, they were in disagreement with the annual-layer thickness of 0.26-0.28 m suggested by Klementyev and others (1988) and used by Kotlyakov and others (1990) for dating the Academy of Sciences ice core drilled in 1986/87. On the other hand, measurements elsewhere in Severnaya Zemlya suggested that annual precipitation decreased with altitude from 0.45 to 0.25 m w.e. a^{-1} (Bryazgin and Yunak, 1988). Assuming, a value of 0.30 m w.e. a^{-1} as average accumulation rate over the entire ice cap (Dowdeswell and others, 2002), we obtained a total accumulation of 1.67 Gt a^{-1}. If, instead, we had used the ice-cap averaged accumulation rate at its upper bound, given by the net accumulation rate at the ice cap crest of 0.46 m w.e. a^{-1} (Fritzsche and others, 2005), the total accumulation over the ice cap would have been 2.56 Gt a^{-1}.

Table S1: Sentinel-1 images used in this study.

Platform	Acquisition date	Polarisation	Orbit number	Pass direction	Cycle number	Slice number
Sentinel-1B	2016-11-06	VV	2831	Descending	23	1
Sentinel-1B	2016-11-09	VV	2875	Descending	23	1
Sentinel-1B	2016-11-30	VV	3181	Descending	25	1
Sentinel-1B	2016-12-03	VV	3225	Descending	25	1
Sentinel-1B	2016-12-12	VV	3356	Descending	26	1
Sentinel-1B	2016-12-15	VV	3400	Descending	26	1
Sentinel-1B	2016-12-24	VV	3531	Descending	27	1
Sentinel-1B	2016-12-27	VV	3575	Descending	27	1
Sentinel-1B	2017-01-05	VV	3706	Descending	28	1
Sentinel-1B	2017-01-08	VV	3750	Descending	28	1
Sentinel-1B	2017-01-17	VV	3881	Descending	30	1
Sentinel-1B	2017-01-20	VV	3925	Descending	30	1
Sentinel-1B	2017-01-29	VV	4056	Descending	30	1
Sentinel-1B	2017-02-01	VV	4100	Descending	30	1
Sentinel-1B	2017-02-13	VV	4275	Descending	31	1
Sentinel-1B	2017-02-22	VV	4406	Descending	32	1
Sentinel-1B	2017-02-25	VV	4450	Descending	32	1
Sentinel-1B	2017-03-06	VV	4581	Descending	33	1
Sentinel-1B	2017-03-09	VV	4625	Descending	33	1
Sentinel-1B	2017-03-18	VV	4756	Descending	34	1
Sentinel-1B	2017-03-21	VV	4800	Descending	34	1
Sentinel-1B	2017-03-30	VV	4931	Descending	35	1
Sentinel-1B	2017-04-02	VV	4975	Descending	35	1
Sentinel-1B	2017-04-11	VV	5106	Descending	36	1
Sentinel-1B	2017-04-23	VV	5281	Descending	37	1
Sentinel-1B	2017-04-26	VV	5325	Descending	37	1
Sentinel-1B	2017-05-05	VV	5456	Descending	38	1
Sentinel-1B	2017-05-17	VV	5631	Descending	39	1
Sentinel-1B	2017-05-20	VV	5675	Descending	39	1
Sentinel-1B	2017-05-29	VV	5806	Descending	40	1
Sentinel-1B	2017-06-01	VV	5850	Descending	40	1
Sentinel-1B	2017-06-10	VV	5981	Descending	41	1
Sentinel-1B	2017-06-13	VV	6025	Descending	41	1
Sentinel-1B	2017-06-22	VV	6156	Descending	42	1
Sentinel-1B	2017-06-25	VV	6200	Descending	42	1
Sentinel-1B	2017-07-07	VV	6375	Descending	43	1
Sentinel-1B	2017-07-16	VV	6506	Descending	44	1
Sentinel-1B	2017-07-19	VV	6550	Descending	44	1
Sentinel-1B	2017-07-31	VV	6725	Descending	45	1
Sentinel-1B	2017-08-09	VV	6856	Descending	46	1
Sentinel-1B	2017-08-12	VV	6900	Descending	46	1
Sentinel-1B	2017-08-21	VV	7031	Descending	47	1
Sentinel-1B	2017-09-02	VV	7206	Descending	48	1
Sentinel-1B	2017-09-05	VV	7250	Descending	48	1
Sentinel-1B	2017-09-14	VV	7381	Descending	49	1
Sentinel-1B	2017-09-17	VV	7425	Descending	49	1
Sentinel-1B	2017-09-26	VV	7556	Descending	50	1
Sentinel-1B	2017-09-29	VV	7600	Descending	50	1
Sentinel-1B	2017-10-08	VV	7731	Descending	51	1
Sentinel-1B	2017-10-11	VV	7775	Descending	51	1
Sentinel-1B	2017-10-20	VV	7906	Descending	52	1
Sentinel-1B	2017-10-23	VV	7950	Descending	52	1
Sentinel-1B	2017-11-01	VV	8081	Descending	53	1
Sentinel-1B	2017-11-04	VV	8125	Descending	53	1
Sentinel-1B	2017-11-16	VV	8300	Descending	54	1

Table S2: ICESat tracks used in this study.

Platform	Acquisition date	Track
ICESat	2003-03-05	20
ICESat	2003-03-21	35
ICESat	2003-03-28	85
ICESat	2003-03-02	100
ICESat	2005-03-02	100
ICESat	2004-03-01	115
ICESat	2005-03-05	154
ICESat	2004-03-04	169
ICESat	2004-03-07	219
ICESat	2004-03-08	234
ICESat	2004-03-11	273
ICESat	2004-03-12	288
ICESat	2004-03-16	338
ICESat	2004-03-17	353
ICESat	2005-03-21	392
ICESat	2004-03-20	407
ICESat	2004-02-21	1320
ICESat	2007-03-15	1335

Table S3: WorldView strips used in this study. See also Fig. S4.

Object ID	Platform	Acquisition date	Function
52913	WorldView-1	2012-05-01	DEM differencing
52915	WorldView-1	2012-05-11	DEM differencing
54035	WorldView-1	2013-07-01	DEM differencing
58189	WorldView-2	2013-07-01	DEM differencing
56797	WorldView-2	2016-05-10	ICESat-DEM differencing and DEM differencing
59961	WorldView-3	2016-05-11	ICESat-DEM differencing and DEM differencing
56205	WorldView-2	2016-06-22	ICESat-DEM differencing
52027	WorldView-1	2016-07-13	ICESat-DEM differencing
59867	WorldView-3	2016-07-14	ICESat-DEM differencing and DEM differencing
59841	WorldView-3	2016-07-29	ICESat-DEM differencing
52092	WorldView-1	2016-07-30	ICESat-DEM differencing
59897	WorldView-3	2016-07-30	ICESat-DEM differencing

Table S4: Partition of mass balance into climatic mass balance and frontal ablation for the drainage basins of the Academy of Sciences Ice Cap. The climatic mass balance has been derived from WorldView-WorldView DEM differencing for 2012/13-2016, except for the basins marked with an asterisk, for which ICESat-WorldView DEM differencing for 2004-2016 has been used. The frontal ablation data correspond to the period November 2016-November 2017.

Drainage Basin	$\dot{M}$		$\dot{B}$		$\dot{D}$	
	Gt a^{-1}	m w.e. a^{-1}	Gt a^{-1}	m w.e. a^{-1}	Gt a^{-1}	m w.e. a^{-1}
North*	-0.05	-0.04	-0.05	-0.04	0	0
West*	0.05	0.05	0.11	0.11	-0.06	-0.06
A	-0.07	-0.11	-0.04	-0.04	-0.03	-0.06
B	-0.21	-0.52	-0.03	-0.07	-0.18	-0.44
South*	-0.02	-0.18	0.02	0.23	-0.04	-0.46
BC	-0.30	-1.09	0.11	0.4	-0.41	-1.49
Southeast*	-0.05	-0.13	0.03	0.08	-0.08	-0.21
C	-0.71	-0.86	-0.02	-0.02	-0.69	-0.83
D	-0.36	-0.76	0.08	0.17	-0.44	-0.93
Ice Cap total	-1.72	-0.31	0.21	0.04	-1.93	-0.35

Table S5: Mass balance for the main drainage basins of the Academy of Sciences Ice Cap and over different periods. Basin North here groups the basins North and West, and 'Others' groups the basins South, BC and Southeast. These names are used for compatibility with Moholdt and others (2012). The values used for computing the 'Ice Cap total' in this study are marked with an asterisk, i.e. we have taken the values for 2012/13-2016 and, when unavailable, those for 2004-2016.

|	Moholdt and others (2012)		This study	
			ICESat-WV	WV-WV
Drainage Basin	1988-2006 (m w.e. a^{-1})	2003-2009 (m w.e. a^{-1})	2004-2016 (m w.e. a^{-1})	2012/13-2016 (m w.e. a^{-1})
Basin north	0.03±0.18	0.07±0.06	0±0.08*	-
A	0.14±0.23	0.14±0.09	−0.09±0.09	−0.11±0.10*
B	−1.13±0.28	−0.23±0.12	−0.25±0.10	−0.52±0.16*
C	−2.30±0.23	−0.86±0.09	−0.90±0.13	−0.86±0.23*
D	−1.57±0.26	−1.11±0.11	−0.92±0.12	−0.76±0.19*
Others	−0.29±0.23	−0.02±0.09	−0.53±0.15*	-
Ice Cap total	−0.55±0.16	−0.19±0.05	−0.31±0.12	
	−3.06±0.89 Gt a^{-1}	−1.06±0.28 Gt a^{-1}	−1.72±0.67 Gt a^{-1}	
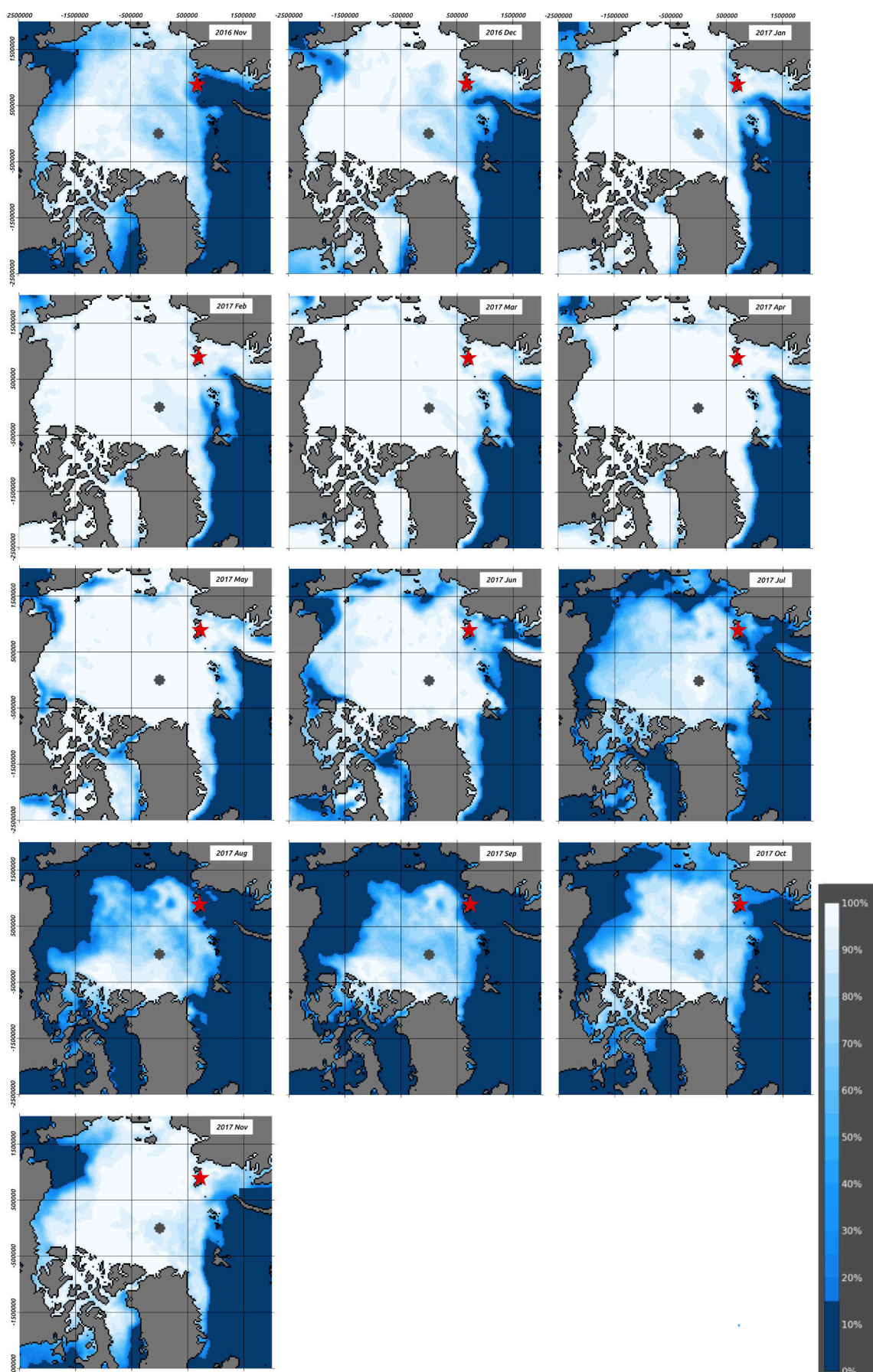
Fig. S1: Monthly-averaged Arctic sea-ice concentration, November 2016-November 2017. NSIDC Sea Ice Polar Stereographic North projection. The location of Severnaya Zemlya is marked with a red star.
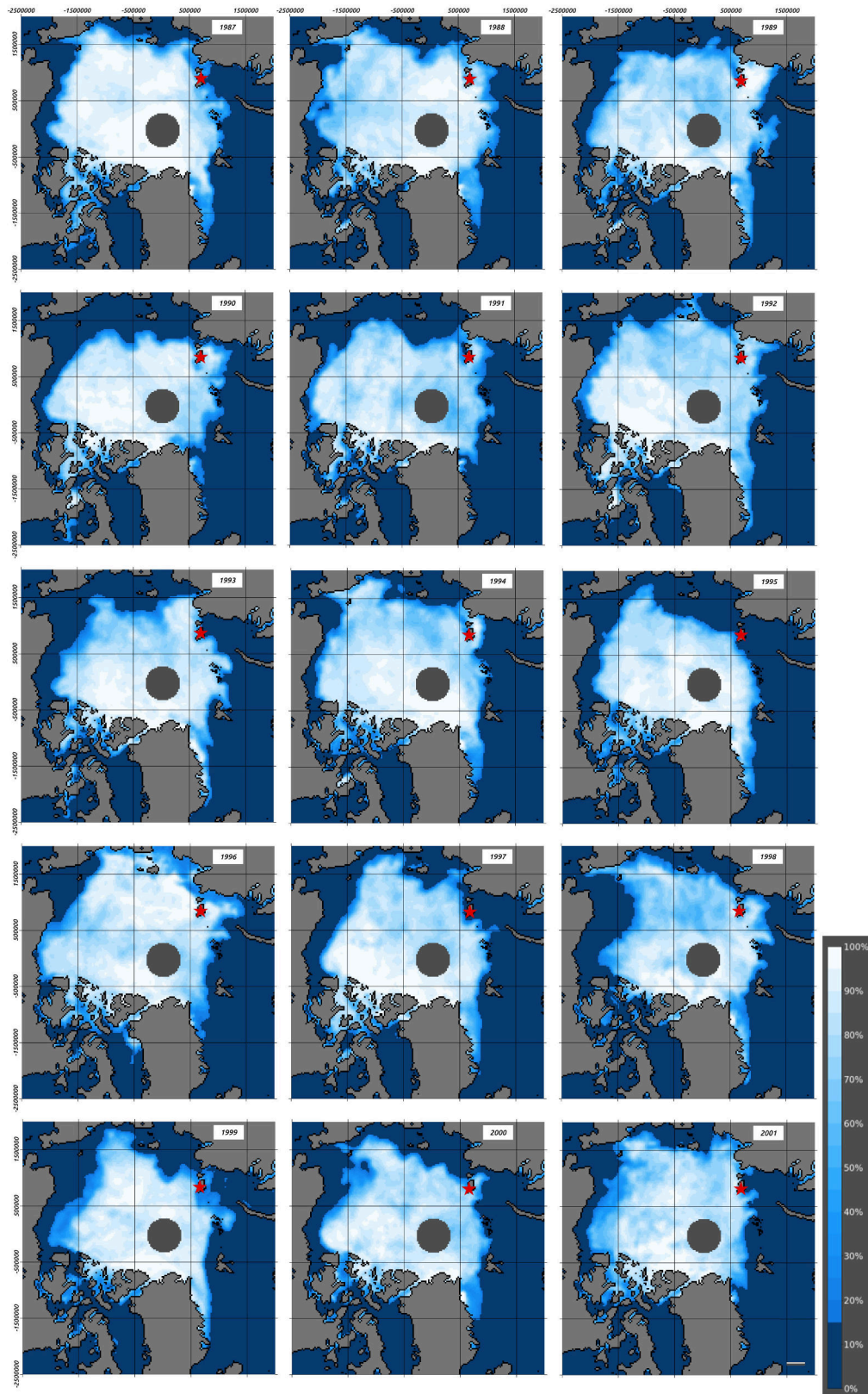
Fig. S2: (a) End of September Arctic sea-ice concentration for the period September 1987-September 2001. NSIDC Sea Ice Polar Stereographic North projection. The location of Severnaya Zemlya is marked with a red star.
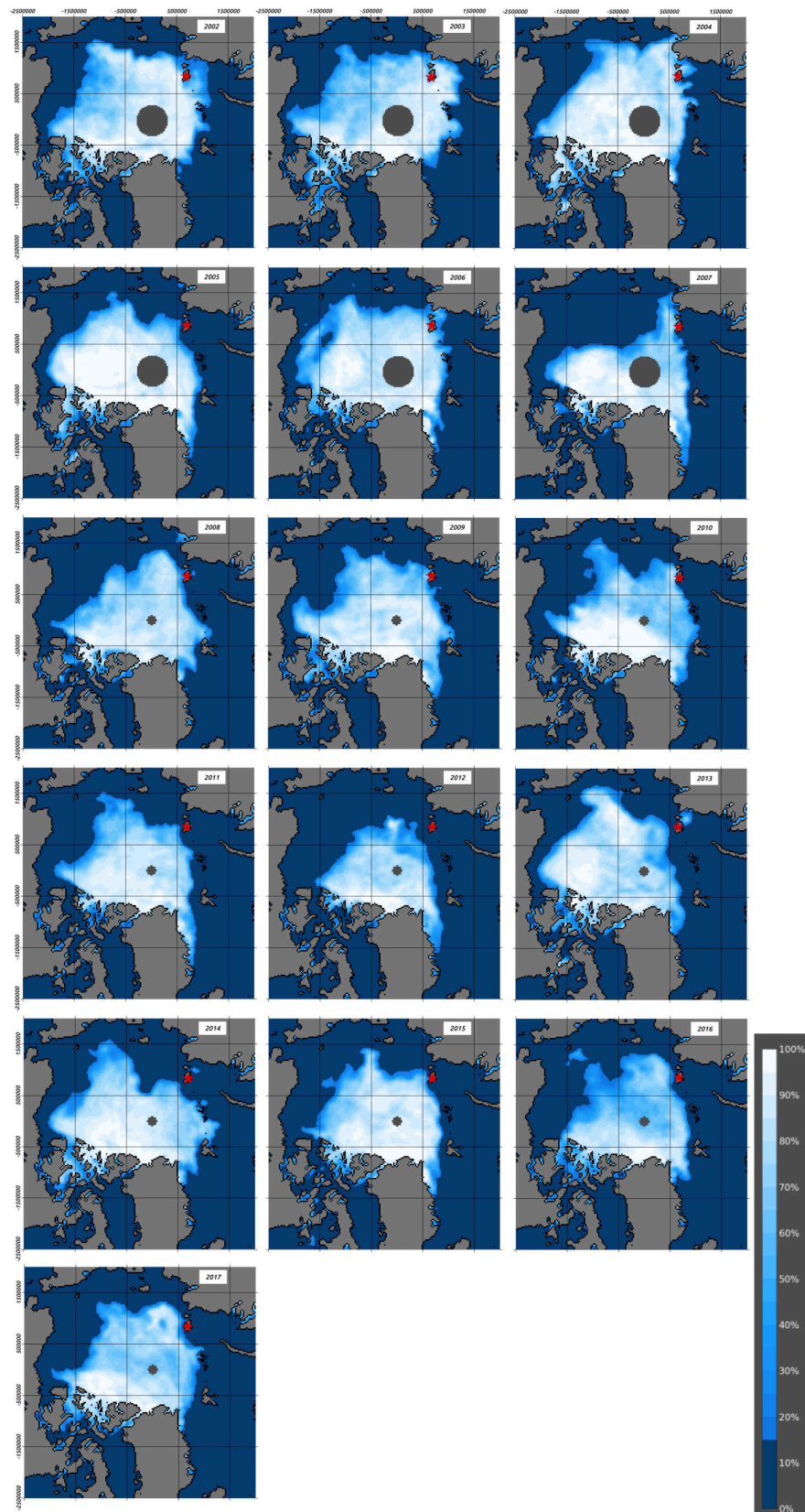
Fig. S2: (b) End of September Arctic sea-ice concentration for the period September 2002-September 2017. NSIDC Sea Ice Polar Stereographic North projection. The location of Severnaya Zemlya is marked with a red star.

Fig. S3: (a) Summer and (b) year-averaged air temperatures from 1987-2017 over Northern Komsomolets Island (from NCEP/NCAR Reanalysis 1 data). Surface temperatures of the closest grid point to the geographic centre of Severnaya Zemlya are used to calculate the values shown in this figure.
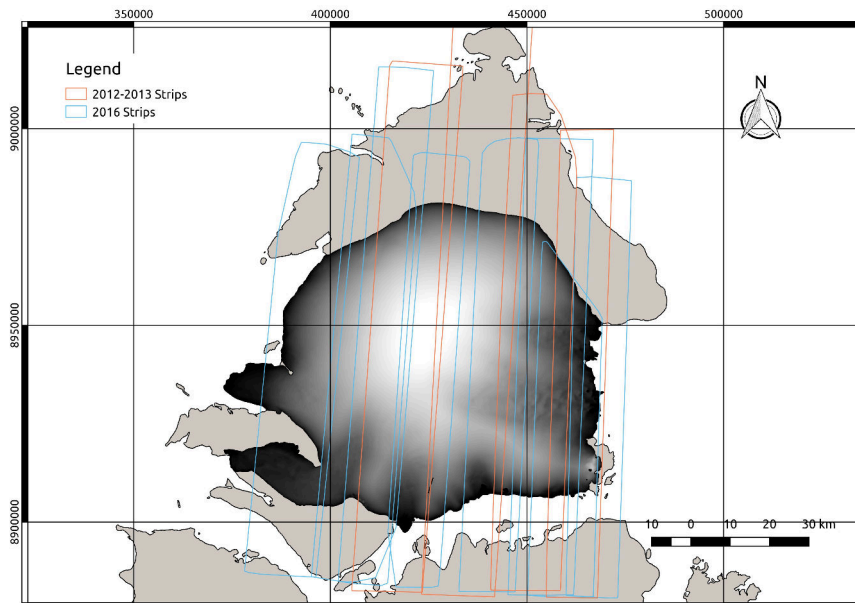
Fig. S4: WorldView strips used in this study.
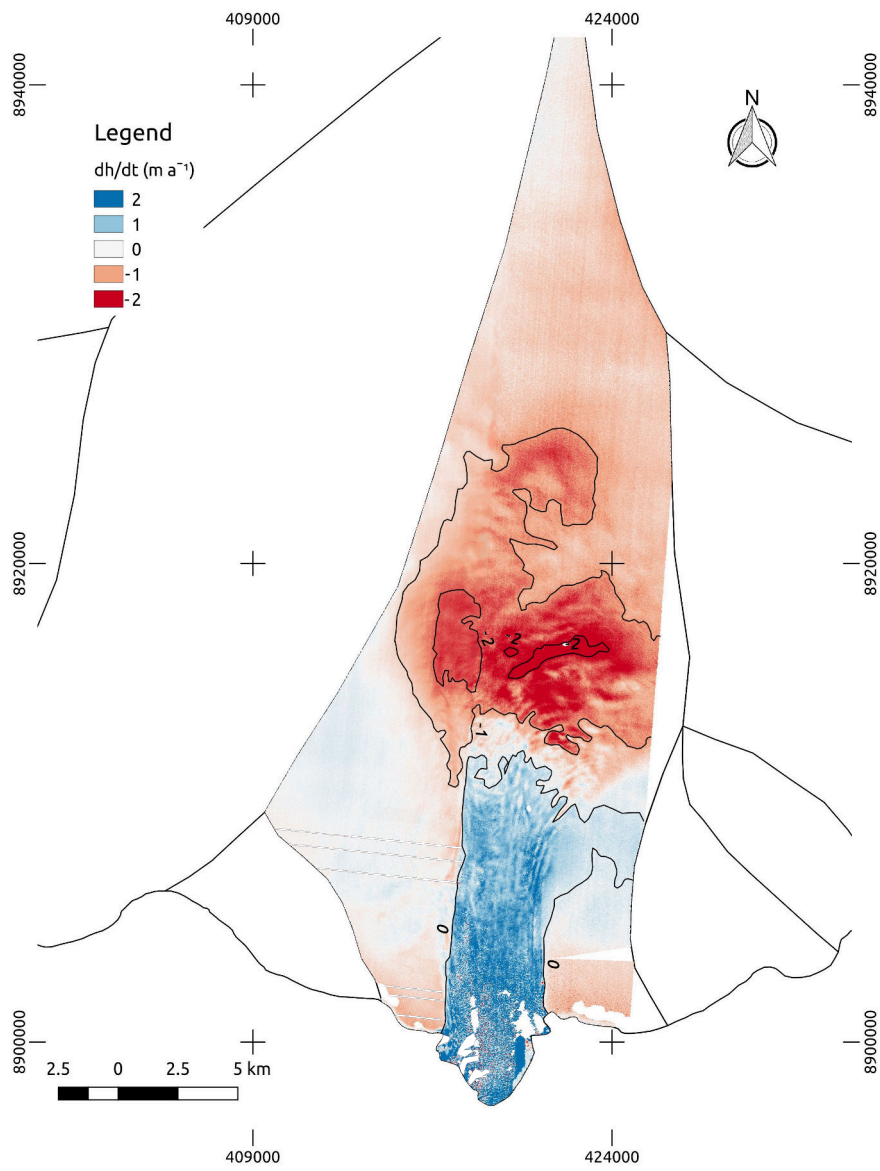
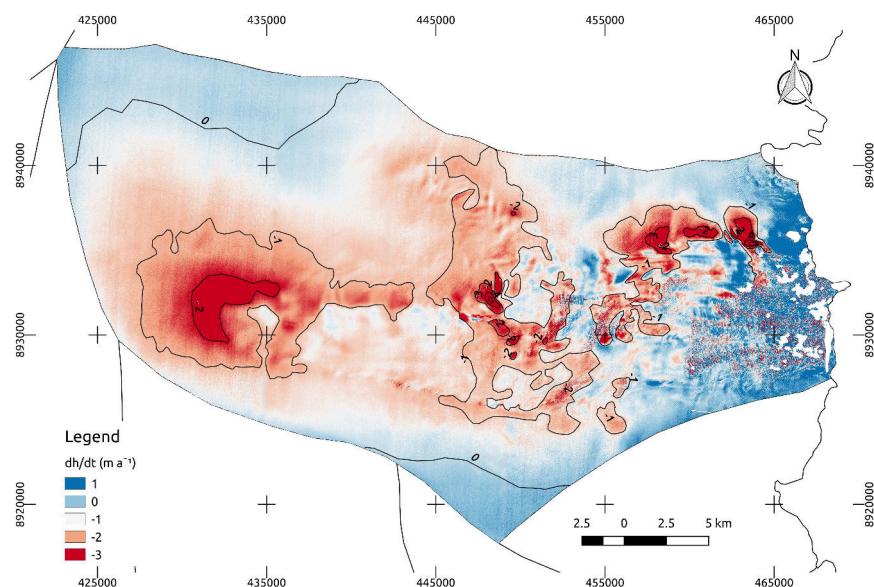Fig. S5: Surface elevation changes WorldView-WorldView (2012/13-2016) for Basin B.

Fig. S6: Surface elevation changes WorldView-WorldView (2012/13-2016) for Basin C.
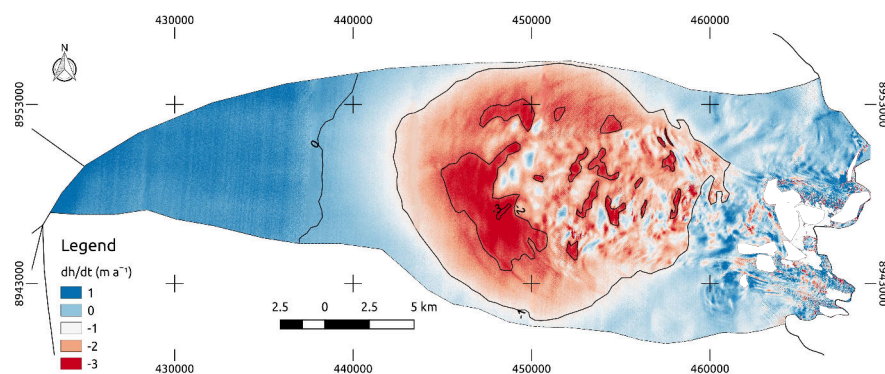

Fig. S7: Surface elevation changes WorldView-WorldView (2012/13-2016) for Basin D.

REFERENCES

Bougamont M, Price S, Christoffersen P and Payne AJ (2011) Dynamic patterns of ice stream flow in a 3-D higher-order ice sheet model with plastic bed and simplified hydrology. *Journal of Geophysical Research*, **116**(F4) (doi: 10.1029/2011jf002025)

Bryazgin NN and Yunak RI (1988) Air temperature and precipitation on Severnaya Zemlya during ablation and accumulation periods, in geographical and glaciological studies in polar countries (in russian). *Gidrometeoizdat, St. Petersburg*, 7081

Dowdeswell JA and 10 others (2002) Form and flow of the Academy of Sciences Ice Cap, Severnaya Zemlya, Russian High Arctic. *J. Geophys. Res.*, **107**(B4), EPM 5–1–EPM 5–15 (doi: 10.1029/2000jb000129)

Fischer UH and Clarke GK (2001) Review of subglacial hydro-mechanical coupling: Trapridge Glacier, Yukon territory, Canada. *Quaternary International*, **86**(1), 29–43 (doi: 10.1016/s1040-6182(01)00049-0)

Francis JA (2013) The where and when of wetter and drier: disappearing Arctic sea ice plays a role. *Environmental Research Letters*, **8**(4), 041002 (doi: 10.1088/1748-9326/8/4/041002)

Fritzsche D and 6 others (2002) A new deep ice core from Akademii Nauk Ice Cap, Severnaya Zemlya, Eurasian Arctic: first results. *Annals of Glaciology*, **35**, 25–28 (doi: 10.3189/172756402781816645)

Fritzsche D and 6 others (2005) A 275 year ice-core record from Akademii Nauk Ice Cap, Severnaya Zemlya, Russian Arctic. *Annals of Glaciology*, **42**, 361–366 (doi: 10.3189/172756405781812862)

Hansen J, Ruedy R, Sato M and Lo K (2010) Global surface temperature change. *Reviews of Geophysics*, **48**(4) (doi: 10.1029/2010rg000345)

Klementyev O, Korotkov I and Nikolaev V (1988) Glaciological studies on the ice domes of Severnaya Zemlya in 1987-1988. *Mater. Glyatsiol. Issled.*, **63**, 25–26

Kotlyakov VM, Zagorodnov VS and Nikolayev VI (1990) Drilling on ice caps in the Soviet Arctic and on Svalbard and prospects of ice core treatment, in Arctic research: Advances and prospects. *Proceedings of the Conference of Arctic and Nordic Countries on Coordination of Research in the Arctic, Leningrad, December 1988*, **2**, 5–18

Kuhn M (2000) Severnaja automatic weather station data (Severnaja Zemlja). in the response of Arctic ice mass to climate change (ICEMASS). third year report (January–December 2000). *European Commission, Framework IV, Environment and Climate Research Programme (DG XII), contract ENV4-CT970490. Oslo, University of Oslo*, 7–87–14

Moholdt G, Heid T, Benham T and Dowdeswell JA (2012) Dynamic instability of marine-terminating glacier basins of Academy of Sciences Ice Cap, Russian High Arctic. *Annals of Glaciology*, **53**(60), 193–201 (doi: 10.3189/2012aog60a117)

Opel T and 7 others (2009) 115 year ice-core data from Akademii Nauk Ice Cap, Severnaya Zemlya: high-resolution record of Eurasian Arctic climate change. *Journal of Glaciology*, **55**(189), 21–31 (doi: 10.3189/002214309788609029)

Opel T, Fritzsche D and Meyer H (2013) Eurasian Arctic climate over the past millennium as recorded in the Akademii Nauk ice core (Severnaya Zemlya). *Climate of the Past*, **9**(5), 2379–2389 (doi: 10.5194/cp-9-2379-2013)

Rennermalm AK, Smith LC, Stroeve JC and Chu VW (2009) Does sea ice influence Greenland ice sheet surface-melt? *Environmental Research Letters*, **4**(2), 024011 (doi: 10.1088/1748-9326/4/2/024011)

Serreze MC, Barrett AP and Stroeve J (2012) Recent changes in tropospheric water vapor over the arctic as assessed from radiosondes and atmospheric reanalyses. *Journal of Geophysical Research: Atmospheres*, **117**(D10), n/a–n/a (doi: 10.1029/2011jd017421)

Stroeve JC, Serreze MC, Holland MM, Kay JE, Malanik J and Barrett AP (2011) The Arctic's rapidly shrinking sea ice cover: a research synthesis. *Climatic Change*, **110**(3-4), 1005–1027 (doi: 10.1007/s10584-011-0101-1)

Tulaczyk S, Kamb WB and Engelhardt HF (2000) Basal mechanics of Ice Stream B, West Antarctica: 1. till mechanics. *Journal of Geophysical Research: Solid Earth*, **105**(B1), 463–481 (doi: 10.1029/1999jb900329)

Willis IC (1995) Intra-annual variations in glacier motion: a review. *Progress in Physical Geography: Earth and Environment*, **19**(1), 61–106 (doi: 10.1177/030913339501900104)

Zhao M, Ramage J, Semmens K and Obleitner F (2014) Recent ice cap snowmelt in Russian High Arctic and anti-correlation with late summer sea ice extent. *Environ. Res. Lett.*, **9**(4), 045009 (doi: 10.1088/1748-9326/9/4/045009)